PHYSICAL REVIEW B **77**, 060102(R) (2008)

Charge-transfer transitions in mixed-valent multiferroic $TbMn_2O_5$

A. S. Moskvin[1] and R. V. Pisarev[2]
[1]*Ural State University, 620083 Ekaterinburg, Russia*
[2]*A. F. Ioffe Physico-Technical Institute of RAS, 194021, St.-Petersburg, Russia*

(Received 10 December 2007; revised manuscript received 18 January 2008; published 26 February 2008)

Optical response of mixed-valent manganite $TbMn_2O_5$ is studied in the spectral range from 0.6 to 5.8 eV in order to reveal the charge-transfer (CT) transitions responsible for the band-gap structure. Strong increase of optical response for the z and y polarizations and strong anisotropy with a relation $\epsilon_{2x} < \epsilon_{2y} < \epsilon_{2z}$ are found. These findings agree with the theoretical analysis derived from the orientation of the $Mn^{3+}O_5$ pyramids in the unit cell and points to the one-center p-d CT transitions as the main contributors to the spectral weight. We argue that the CT processes are accompanied by giant electric-dipole fluctuations and therefore may be a source of large electric polarization of $Mn^{3+}O_5$ pyramids due to the parity-breaking Mn^{3+}-Mn^{4+} isotropic exchange interaction.

DOI: 10.1103/PhysRevB.77.060102 PACS number(s): 78.20.Ci, 75.47.Lx, 71.20.Ps

Multiferroic materials that possess several order parameters and exhibit coupling between electrical polarization, spontaneous magnetization, and/or spontaneous strain have been actively studied in the 1960s and 1970s. Only very few materials of this kind have been found and in most cases coupling between order parameters was not strong enough to find any technological applications. However, progress in the recent two decades in the technology of making new materials and structures with controllable properties and the development of new methods for computing electronic and magnetic structures triggered the revival of interest to multiferroics, see, e.g., Refs. 1–3.

Manganese oxides on the basis of $Mn^{3+}(3d^4)$ and $Mn^{4+}(3d^3)$ ions hold a distinguished position among known multiferroics. Hexagonal manganites $RMnO_3$ (R = Y, Dy–Lu)[4] and orthorhombic perovskite-type manganites $RMnO_3$ (R=La–Dy)[5] with the Jahn-Teller Mn^{3+} ions became the most popular objects for the studies of the gigantic magnetoelectric effect and strong dielectric anomalies at the magnetic phase transitions. A lot of attention has been devoted in recent years to the orthorhombic mixed-valent Mn^{3+}-Mn^{4+} manganites RMn_2O_5 (R=Tb, Dy, *et al.*), where giant magnetoelectric effects have been observed.[6,7] Despite experimental and theoretical efforts, the microscopic mechanism of giant magnetoelectric effects is still a matter of debate. One of the main controversial points concerns the actual origin and microstructure of local electric polarizations.

In this paper we report the results of theoretical and experimental investigations of optical response for $TbMn_2O_5$ single crystals aimed to study the charge-transfer (CT) transitions, optical anisotropy, and uncover electronic states as potential contributors to giant multiferroicity. A search for a link between phonon spectra and multiferroicity in RMn_2O_5 was recently undertaken in Refs. 8–11. However, no experimental reports are available on the near-band-gap electronic structure of these materials, which is of primary importance for constructing appropriate Hubbard models and obtaining an adequate theoretical description of the multiferroic properties.

The mixed-valent compounds RMn_2O_5 crystallize in the orthorhombic structure, space group $Pbam$,[9,12] see Fig. 1. The $Mn^{4+}O_6$ octahedra share edges to form infinite chains along the z axis. Every two $Mn^{3+}O_5$ pyramids, doubly linked by oxygens, form a dimer unit Mn_2O_{10}. Four $Mn^{4+}O_6$ octahedra chains are linked by a dimer unit in the xy planes through two oxygen ions. The fourfold symmetry axis in the $Mn^{3+}O_5$ pyramids lies in the xy plane at an angle of about $\pm 24°$ to the x axis. We note that the Jahn-Teller Mn^{3+} ions prefer pyramid sites, whereas Mn^{4+} ions strongly prefer octahedral sites due to crystal-field stabilization energy $-12Dq$.[13] These preferences may explain the fact that the mixed-valent manganites RMn_2O_5 are good insulators.

The optical complex dielectric function $\varepsilon = \varepsilon_1 - i\varepsilon_2$ of single crystalline samples of $TbMn_2O_5$ was studied with the use of a variable-angle spectroscopic ellipsometer in the range from 0.6 to 5.8 eV, as described elsewhere.[14,15] The technique of ellipsometry provides significant advantages over conventional reflection methods because (i) it does not require reference measurements, and (ii) optical complex dielectric functions $\varepsilon = \varepsilon_1 - i\varepsilon_2$ are obtained directly without the Kramers-Krönig transformation. $TbMn_2O_5$ is an optically biaxial material and the measurements were done in reflection from several polished natural surfaces of a single crystalline sample with incident light polarizations along the $x(a)$, $y(b)$,

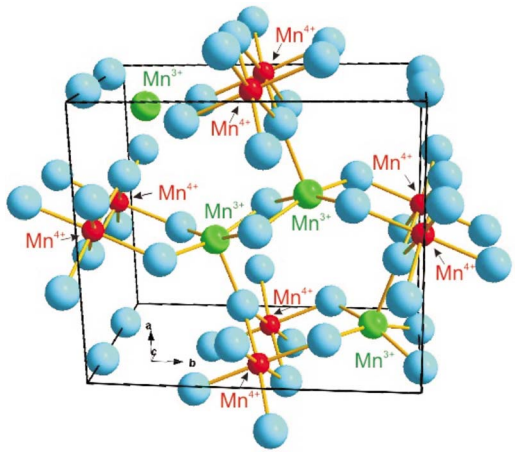

FIG. 1. (Color online) The crystal structure and Mn-O bondings in $TbMn_2O_5$. For clarity, terbium ions are omitted.

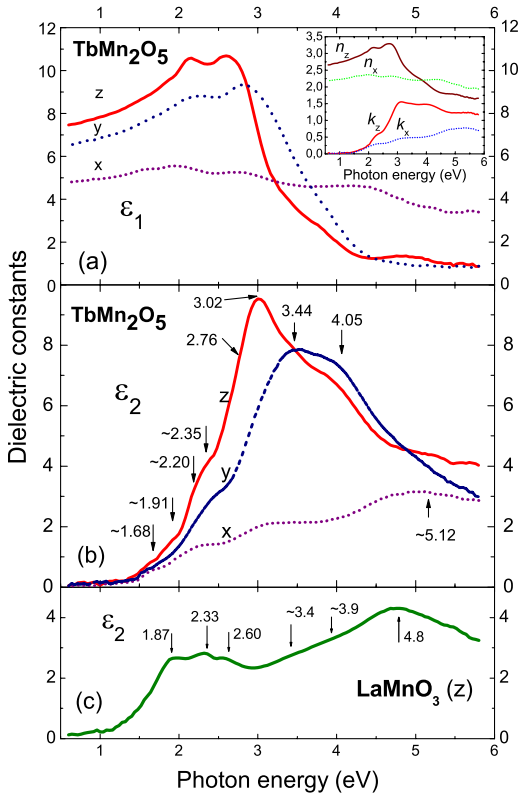

FIG. 2. (Color online) (a) Real ϵ_1 and (b) imaginary ϵ_2 parts of the dielectric function in $TbMn_2O_5$. Plot (c) shows ϵ_2 function in $LaMnO_3$ where Mn^{3+} ions are only in octahedral positions and there are no Mn^{4+} ions.

and $z(c)$ crystallographic axes. Optical absorption near the band gap was studied with the use of a spectrophotometer.

Figure 2 shows (a) ε_1 and (b) ε_2 room temperature spectra of $TbMn_2O_5$ for three main light polarizations. For comparison we measured the ε_2 spectrum [see Fig. 2(c)] of the perovskite-type manganite $LaMnO_3$, where Mn^{3+} ions are only in octahedral positions.[16] In $TbMn_2O_5$ the most intense absorption (see ε_2 spectra) is observed for light polarization along the z axis, while the less intense is observed for light polarization along the x axis. This optical anisotropy gives rise to giant linear dichroism and birefringence, see the inset to Fig. 2(a). Figure 3 shows the temperature dependence of the absorption edge of $TbMn_2O_5$ near 1.4 eV for the light polarized along the x axis. The edge shifts to a higher energy when temperature is decreased, as shown in the inset. The band gap arises due to the lowest energy oscillator distinctly seen at about 1.7 eV. At higher energy the visibly split oscillators at 2.26–2.38 eV are seen in all polarizations. The strongest peak of $\epsilon_{2z} \approx 10$ is located at 3.02 eV while for the two other polarizations it is several times weaker. Slightly weaker peaks of $\epsilon_{2y} \approx 8$ are found at 3.44 and 4.05 eV. A relatively weak maximum of $\epsilon_{2x} \approx 3$ is revealed at 5.0 eV. The band at 3.9–4.0 eV is equally intensive both in the y and z polarizations. However, it is hardly distinguishable for the x polarization. The band at 5.0 eV is distinctly visible only in the x polarization, whereas for the other polarizations it forms a structureless feature.

Intensive and broad absorption bands in $TbMn_2O_5$ point

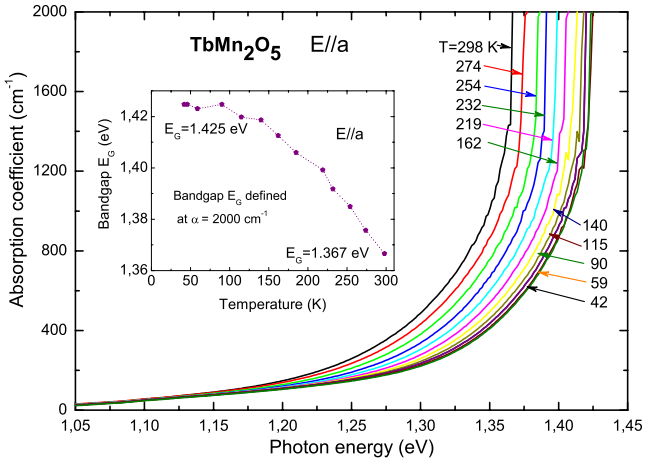

FIG. 3. (Color online) Near-band-gap absorption spectra for the x polarization of light. Inset shows temperature dependence of the band gap defined at $\alpha = 2000\ cm^{-1}$. Similar behavior was observed for the z polarization.

to the p-d and d-d CT transitions as a main mechanism of optical response. A semiquantitative description of the p-d transitions in octahedral $Mn^{4+}O_6$ centers can be done with the use of a diagram of molecular orbitals and energies shown in Fig. 4 and the model theory for $LaMnO_3$.[17] All the p-d CT transitions in octahedral $3d$ centers can be subdivided into (i) dipole-forbidden ones $t_{1g}(\pi) \rightarrow e_g, t_{2g}$; (ii) weak dipole-allowed π-σ transitions $t_{2u}(\pi) \rightarrow e_g$ and $t_{1u}(\pi) \rightarrow e_g$; (iii) strong dipole-allowed σ-σ and π-π CT transitions, $t_{1u}(\sigma) \rightarrow e_g$ and $t_{2u}(\pi), t_{1u}(\pi) \rightarrow t_{2g}$, respectively. At variance with the Jahn-Teller $Mn^{3+}O_6$ centers in $LaMnO_3$, the p-d CT transitions in the near octahedral $Mn^{4+}O_6$ centers in $TbMn_2O_5$ with the S-type ground state ${}^4A_{2g}(t_{2g}^3)$ are remarkable for the weak anisotropy. For the Mn^{3+} sublattice in $TbMn_2O_5$ we should consider strong parity-breaking effects

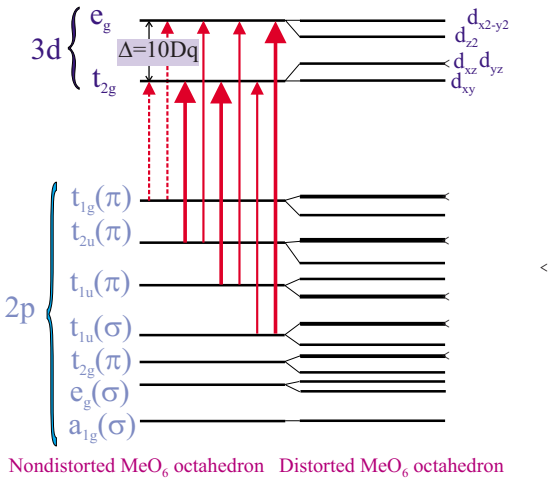

FIG. 4. (Color online) The diagram of molecular orbitals for the MeO_6 octahedral center. The O $2p$-Me $3d$ charge-transfer transitions are shown by arrows: strong dipole-allowed σ-σ and π-π by the thick solid arrows; weak dipole-allowed π-σ and σ-π by the thin solid arrows; weak dipole-forbidden low-energy transitions by thin dashed arrows, respectively.

and tetragonal distortions due to the fivefold pyramidal oxygen surrounding. Nevertheless, the scheme in Fig. 4 may be used for a qualitative analysis of the *p-d* CT transitions in $Mn^{3+}O_5$ pyramids as well. The most important impact of the tetragonality consists in large d_{z^2}-$d_{x^2-y^2}$ splitting on the order of 1 eV due to a strong decrease of the d_{z^2}-level energy. In addition, we deal with a strong rearrangement of electron states for neighboring oxygen ions. For taking into account this rearrangement careful band-model calculations are necessary. Nevertheless, simple symmetry considerations allow us to obtain very instructive information regarding the polarization properties of the *p-d* CT transitions in MnO_5 pyramidal clusters. Let us address the polarization properties of the main dipole-allowed one-center *p-d* CT transition $t_{1u}(\sigma) \rightarrow e_g$. The $t_{1u(x,y)}(\sigma) \rightarrow d_{x^2-y^2}$ transition is only allowed for the light polarized within the basal plane of MnO_5 pyramids, while the $t_{1uz}(\sigma) \rightarrow d_{z^2}$ transition is only allowed for the light polarized along the local tetragonal axis of the pyramids. The former transition generates the absorption band with polarization properties in the crystal *xyz* coordinates as follows:

$$SW_x:SW_y:SW_z = \sin^2\theta:\cos^2\theta:1 = 0.16:0.84:1.00, \quad (1)$$

where $SW_{x,y,z}$ are spectral weights for the respective light polarization, and $\theta \approx \pm 24°$ is the angle between the tetragonal axis of MnO_5 pyramids and the crystal *x* axis. The latter transition generates the absorption band with polarization properties as follows:

$$SW_x:SW_y:SW_z = \cos^2\theta:\sin^2\theta:0 = 0.84:0.16:0. \quad (2)$$

Expressions (1) and (2) can be used for a reliable assignment of the *p-d* CT transitions in the $Mn^{3+}O_5$ pyramids. We note that the integral spectral weights for the one-center *p-d* CT transitions in octahedral MnO_6^{8-} and pyramidal MnO_5^{7-} centers are expected to be of comparable magnitudes.

Let us discuss two-center *d-d* CT transitions that can contribute significantly both to the optical and magnetoelectric response. For instance, in $LaMnO_3$ these transitions lead to an intensive absorption band peaked near 2 eV.[16] The *d-d* CT transition probability amplitude is determined by the respective single-particle transfer integral and the spectral weight can be related to a kinetic contribution to the (super)exchange integral.[16] These integrals depend both on initial and final states, and the Me_1-O-Me_2 bond geometry. Presence of various competing exchange interactions makes the analysis of exchange coupling in $TbMn_2O_5$ a rather complicated task. In the mixed-valent RMn_2O_5 there are four types of the two-center *d-d* CT transitions. The *d-d* transitions in Mn^{3+}-Mn^{3+} pairs, or dimer units Mn_2O_{10},

$$MnO_5^{7-} + MnO_5^{7-} \rightarrow MnO_5^{8-} + MnO_5^{6-} \quad (3)$$

imply the creation of electron MnO_5^{8-} and hole MnO_5^{6-} centers with electron configurations $t_{2g}^3 e_g^2$ and t_{2g}^3, formally related to Mn^{2+} and Mn^{4+}, respectively. The high-spin *d-d* CT transition can be represented as follows:

$$MnO_5^{7-}(t_{2g}^3 e_g^1; {}^5E_g) + MnO_5^{7-}(t_{2g}^3 e_g^1; {}^5E_g) \rightarrow MnO_5^{8-}(t_{2g}^3 e_g^2; {}^6A_{1g}) + MnO_5^{6-}(t_{2g}^3; {}^4A_{2g}). \quad (4)$$

These transitions are only allowed if the polarization vector **E** of the incident light lies within the *xy* plane. The *d-d* CT transitions in Mn^{4+}-Mn^{4+} pairs imply the creation of electron MnO_6^{9-} and hole MnO_6^{7-} centers with electron configurations $t_{2g}^3 e_g^1$ and t_{2g}^2, formally related to Mn^{3+} and Mn^{5+}, respectively. The high-spin *d-d* CT transition can be represented as follows:

$$MnO_6^{8-}(t_{2g}^3; {}^4A_{2g}) + MnO_6^{8-}(t_{2g}^3; {}^4A_{2g}) \rightarrow MnO_6^{9-}(t_{2g}^3 e_g^1; {}^5E_g) + MnO_6^{7-}(t_{2g}^2; {}^3T_{1g}). \quad (5)$$

These transitions are allowed only if **E** is parallel to the *z* axis. The two types of the *d-d* CT transitions in Mn^{4+}-Mn^{3+} pairs imply the creation of electron MnO_6^{9-} and hole MnO_5^{6-} centers with electron configurations $t_{2g}^3 e_g^1$ and t_{2g}^3, formally related to Mn^{3+}, and Mn^{4+} or electron MnO_5^{8-} and hole MnO_6^{7-} centers with electron configurations $t_{2g}^3 e_g^2$ and t_{2g}^2, formally related to Mn^{5+} and Mn^{2+}, respectively. Interestingly, the transfer energy in the former transition does not depend on the *dd* correlation parameter U_d, whereas the latter transition energy includes $2U_d$. At variance with the first two types of *d-d* CT transitions these are polarized in a more complicated way. The quantitative estimates of the spectral weight for the *d-d* CT transitions in $TbMn_2O_5$ show several times weaker effects than those in $LaMnO_3$ due to respective scale of spin ordering temperatures and exchange integrals.

Turning to a comparison of theoretical predictions with our experimental data we should first point to an obvious relation $\epsilon_{2x} < \epsilon_{2y} < \epsilon_{2z}$, which holds almost over the whole spectral range under study. This unambiguously points to the one-center *p-d* CT transitions to the final $d_{x^2-y^2}$ state in MnO_5 pyramids as main contributors to the spectral weight. First, the spectral weights $SW_{x,y,z}$ obey nicely the ratio (1). The strongest bands peaked near 3–4 eV may be attributed to the $t_{1u(x,y)}(\sigma) \rightarrow d_{x^2-y^2}$ transition. It should be noted that the line shape of the band actually depends on the rhombic distortions of $Mn^{3+}O_5$ pyramids lifting the $t_{1ux,y}(\sigma)$ degeneracy. Second, we do not see sizable contributions of any two-center *d-d* CT transitions which are remarkable for their polarization properties. Third, the one-center *p-d* CT transitions in $Mn^{4+}O_6$ octahedra, being remarkable for the weak optical anisotropy, are likely displayed as a rather wide band peaked near 5 eV. It distinctly shows up in ϵ_{2x} where the $Mn^{3+}O_5$ pyramid contribution is strongly suppressed. Below main *p-d* CT bands we find several weak bands which may be related both to a number of weakly allowed *p-d* CT transitions and *d-d* CT transitions. Their unambiguous assignment needs an additional experimental study.

Now we would like to emphasize that the CT processes are certainly accompanied by strong electric dipole fluctuations. The *p-d* and *d-d* CT transitions provide a largest contribution to an electric polarizability of MeO_n clusters that can make them important participants of the effective magnetoelectric coupling in strongly correlated 3*d* oxides. The "multiferroic" manifestation of the *p-d* CT transitions can be clearly demonstrated in the framework of a model theory of exchange-induced electric polarization.[18] We argue that this model suggests a reasonable electronic mechanism of giant multiferroicity. Indeed, in the 3*d* oxides the parity-breaking exchange interaction between metal-oxygen MeO_n clusters

can induce strong electric field resulting in a spin-dependent electric polarization[18] $\mathbf{P}=\Sigma_{ij}\mathbf{\Pi}_{ij}(\mathbf{S}_i\cdot\mathbf{S}_j)$ of the clusters due to the hybridization of the even-parity antibonding t_{2g} and e_g orbitals with purely oxygen odd-parity nonbonding orbitals such as $t_{1u}(\sigma)$, $t_{1u}(\pi)$, $t_{2u}(\pi)$ in MeO_6 clusters. Namely, the latter are believed to be the most efficient partners of the even-parity $3d$ orbitals in forming a strongly polarizable entity. This makes the p-d CT states and transitions $t_{1u}(\sigma),t_{1u}(\pi),t_{2u}(\pi)\rightarrow 3dt_{2g},3de_g$ in strongly correlated $3d$ oxides the most likely participants of the effective magnetoelectric coupling.

In conclusion, the investigation of dielectric functions of single crystalline $TbMn_2O_5$ samples in the region of p-d and d-d charge-transfer transitions allowed us to uncover electronic states responsible for strong increase of optical response and anisotropy. We have found a particularly strong contribution of $Mn^{3+}O_5$ pyramids to electronic polarization. We argue that the p-d CT processes accompanied by giant electric-dipole fluctuations may be a source of large spin-dependent electric polarization of covalently bonded $d_{x^2-y^2}$ state of $Mn^{3+}O_5$ pyramids due to the parity-breaking Mn^{3+}-Mn^{4+} isotropic exchange interaction. For confirmation of effectiveness of this mechanism further theoretical and experimental studies of the near-band-gap states and their variations near magnetic and structural phase transitions would be important.

We thank A. M. Balbashov and V. A. Sanina for $LaMnO_3$ and $TbMn_2O_5$ single crystals, H.-L. Keller for help in making Fig. 1, and Th. Rasing and H.-J. Weber for providing opportunity for optical measurements. The RFBR, NWO, and INTAS are acknowledged for financial support.

[1] M. Fiebig, J. Phys. D **38**, R123 (2005).
[2] D. I. Khomskii, J. Magn. Magn. Mater. **306**, 1 (2006).
[3] W. Eerenstein, N. D. Mathur, and J. F. Scott, Nature (London) **442**, 759 (2006).
[4] M. Fiebig, D. Fröhlich, K. Kohn, S. Leute, T. Lottermoser, V. V. Pavlov, and R. V. Pisarev, Phys. Rev. Lett. **84**, 5620 (2000).
[5] T. Kimura, T. Goto, H. Shintani, T. Arima, and Y. Tokura, Nature (London) **426**, 55 (2003).
[6] N. Hur, S. Park, P. A. Sharma, J. S. Ahn, S. Guha, and S.-W. Cheong, Nature (London) **429**, 392 (2004).
[7] H. Kimura, S. Kobayashi, S. Wakimoto, Y. Noda, and K. Kohn, Ferroelectrics **354**, 77 (2007).
[8] B. Mihailova, M. M. Gospodinov, B. Güttler, F. Yen, A. P. Litvinchuk, and M. N. Iliev, Phys. Rev. B **71**, 172301 (2005).
[9] A. F. García-Flores, E. Granado, H. Martinho, R. R. Urbano, C. Rettori, E. I. Golovenchits, V. A. Sanina, S. B. Oseroff, S. Park, and S.-W. Cheong, Phys. Rev. B **73**, 104411 (2006).
[10] A. Pimenov, A. A. Mukhin, V. Y. Ivanov, V. D. Travkin, A. M. Balbashov, and A. Loidl, Nat. Phys. **2**, 97 (2006).
[11] A. B. Sushkov, R. V. Aguilar, S. Park, S-W. Cheong, and H. D. Drew, Phys. Rev. Lett. **98**, 027202 (2007).
[12] J. A. Alonso, M. T. Casais, M. J. Martinez-Lope, and I. Rasines, J. Solid State Chem. **129**, 105 (1997).
[13] A. B. P. Lever, *Inorganic Electronic Spectroscopy* (Elsevier, Amsterdam, 1984).
[14] A. M. Kalashnikova and R. V. Pisarev, JETP Lett. **78**, 143 (2003).
[15] P. A. Usachev, R. V. Pisarev, A. V. Kimel, A. Kirilyuk, and T. Rasing, Phys. Solid State **43**, 2292 (2005).
[16] N. N. Kovaleva, A. V. Boris, C. Bernhard, A. Kulakov, A. Pimenov, A. M. Balbashov, G. Khaliullin, and B. Keimer, Phys. Rev. Lett. **93**, 147204 (2004).
[17] A. S. Moskvin, Phys. Rev. B **65**, 205113 (2002).
[18] Y. Tanabe, T. Moriya, and S. Sugano, Phys. Rev. Lett. **15**, 1023 (1965).